



A N-self-doped carbon catalyst derived from pig blood for oxygen reduction with high activity and stability

Jian Zhang^a, Qidong Li^b, Chenyu Zhang^a, Liqiang Mai^b, Mu Pan^a, Shichun Mu^{a,*}

^a State Key Laboratory of Advanced Technology for Materials Synthesis and Processing, Wuhan University of Technology, Wuhan 430070, China

^b WUT-Harvard Joint Nano Key Laboratory, Wuhan University of Technology, Wuhan 430070, China



ARTICLE INFO

Article history:

Received 11 January 2015

Accepted 31 January 2015

Available online 1 February 2015

Keywords:

Pig blood

Carbonization

Noble-metal-free catalyst

Oxygen reduction reaction

Low temperature fuel cells

ABSTRACT

A new pig blood-derived N-self-doped carbon catalyst is successfully fabricated with aid of metal iron in the synthetic process. The prepared catalyst shows an excellent oxygen reduction reaction (ORR) performance with high onset potential ($E_{onset} = -0.04$ V) and half-wave potential ($E_{1/2} = -0.16$ V), which very approaches that of the commercial Pt/C catalyst ($E_{onset} = -0.03$ V, $E_{1/2} = -0.14$ V) in alkaline electrolytes. Particularly, the catalyst possesses a significantly superior stability and immunity for methanol crossover and CO poisoning than that of Pt/C. The synthetic method is simple and cost-effective, providing a great opportunity to produce an eco-friendly and cheaper non-platinum fuel cell catalyst by using abundant natural biological resources.

© 2015 Elsevier Ltd. All rights reserved.

1. Introduction

Low temperature fuel cells (LTFCs) with high energy and power density are attracting widespread attention as green and efficient alternative energy sources in future [1–3]. However, as the best catalytic activity for ORR, expensive platinum (Pt) or Pt based catalysts usually have to be used owing to the sluggish ORR under ambient condition. Meanwhile, such catalysts still suffer from poor stability and serious intermediate tolerance, such as CO poisoning and methanol crossover [4], severely confining the commercialization of LTFCs. Consequently, developing high cost-effective and durable catalysts for efficient oxygen reduction to replace Pt-based catalysts has become one of the most attractive topics in fuel cell fields.

Recently the carbon-based catalyst has been confirmed as one of the most promising alternatives to Pt-based catalysts because carbon is more abundant and much less expensive than Pt. Moreover, the introduction of heteroatoms (N, B, P, S, F, Fe or Co et. al) atoms into sp^2 -hybridized carbon frameworks can effectively modify their non-uniform distribution of the spin and atomic charge density, which is very important for oxygen adsorption and activity enhancement [4–9]. These heteroatom-doped carbon materials not only possess a high catalytic activity, but have long-term stability and excellent intermediate tolerance compared to Pt-based catalysts in LTFCs [2,10,11]. However, such materials are

either expensive or harmful to human health because most of them derive from fossil, hazardous inorganic or organic chemicals even ammonia, [1,2,12,13]. Besides, their preparation is typically carried out with complex procedures or stringent conditions. Therefore, developing high cost-effective N-doped carbon catalysts with excellent functional properties by using non-toxic and cheaper renewable resources, is eagerly expected.

Animal blood, especially pig blood (PB) is one of most meat industry byproducts around the world. Only in China, more than 2.5 million tons of PB is produced per year [14,15], and predominantly used as fodder or thrown away as wastes, seriously debasing the value of PB. Nevertheless, PB as a cheap biological N-enriched (18% protein) renewable resource [14,15], is potential to be applied to fabricate a new N-self-doped carbon catalyst with high electrocatalytic performance only by adding extremely low amount of iron. Although several doped carbon materials generated from animal resources were studied in the literature [16,17], to the best of our knowledge, there is a rare report on high cost-effective fabrication of N-self-doped carbon as a high activity catalyst for ORR that very approaches the commercial Pt/C catalyst.

2. Experimental Section

2.1. Materials

Pig blood (PB) was collected from local slaughter plant. Ferric chloride ($FeCl_3 \cdot 6H_2O$) and potassium hydroxide (KOH) were purchased from Sinopharm Chemical Reagent, and Nafion solution (5 wt %) was obtained from Sigma-Aldrich. All the chemicals were

* Corresponding author. Tel.: +86 27 87651837; fax: +86 27 87879468.
E-mail address: msc@whut.edu.cn (S. Mu).

used as delivered without further treatment. Ultra pure water was obtained from a Lab. ultra pure water filter system with a resistivity $\geq 18 \text{ M}\Omega \text{ cm}^{-1}$. Rotating disk electrodes of glassy carbon (RDE, 5 mm in diameter) were purchased from Tianjin Aida Hengsheng Tech. Co., China.

2.2. Material syntheses

PB was diluted with an equal amount of water. And then 0.1 mol L^{-1} FeCl_3 solution was added drop-wise to the above suspension and kept stirring for 2 h (Fe: PB = 1: 25, wt. %). The mixture was cooked in a water bath (100°C , 2 hours), and then dried in an air-circulating oven at 80°C to obtain the precursor. The precursor was carbonized at 900°C in an inert atmosphere. Temperature settings were as follows: the precursor was performed at 200°C for 0.5 h at a heating rate of $2^\circ\text{C}/\text{min}$ in an inert atmosphere, subsequently it was performed at 900°C for 2 h at a heating rate of $5^\circ\text{C}/\text{min}$ in an inert atmosphere, and then the sample was cooled under the same atmosphere from 900°C to 60°C . After that, the black carbon was transferred into a milling tank and grinded on a planetary ball mill (Nanjing Chishun Science & Technology Co., Ltd. PM) for 4 h at 250 rpm. The resulting carbon powder was pre-leached in 0.5 M H_2SO_4 at 80°C for 8 h to remove unstable and inactive species from the catalyst, followed by thoroughly washed in de-ionized water and absolute ethyl alcohol, and then dried at 80°C under vacuum. Finally, the product was heat-treated again at 900°C for 2 h at a heating rate of $5^\circ\text{C}/\text{min}$ in nitrogen atmosphere to obtain the CPB-Fe. For comparison, the sample of CPB (without iron), was also obtained by the similar way. The specific synthesis process of CPB-Fe catalyst is shown in Fig. S1 (Supplementary Information, SI).

2.3. Physical and Chemical Characterizations

The morphology and structure of the samples were further analyzed using JSM-7100F field emission scanning electron

microscope (FESEM) and JEM-2100 high-resolution transmission electron microscopy (HRTEM). Nitrogen adsorption-desorption isotherms were recorded at 78 K with a Micromeritics ASAP 2020 Brunauer Emmett Teller (BET) analyzer. The electronic structure of surfaces for the catalyst was performed using VG-Multi-lab2000 X-ray photoelectron spectroscopy (XPS). Accurate iron content of these catalysts was performed using inductively coupled plasma-atomic emission spectrometry (ICP-AES). Raman spectroscopy was carried out on a Renishaw using the Ar ion laser with an excitation wavelength of 514.5 nm.

2.4. Electrochemical characterizations

The working electrode was prepared by loading 0.6 mg cm^{-2} sample on a glassy carbon electrode. Prior to preparing the working electrode, a homogeneous catalyst ink was made by mixture of 5.0 mg catalyst, 25 μL Nafion ionomer solution (5 wt%, DuPont) and 0.475 mL ultra pure water. As a benchmark, the commercial Pt/C (20 wt%, JM) catalyst was also spread onto the surface of a glassy carbon disk electrode in a similar way, the Pt loading was $20 \mu\text{g Pt cm}^{-2}$. All the electrochemical properties of the catalysts were measured using a conventional three compartment electro-chemical cell in 0.1 M KOH aqueous solution. Besides the prepared working electrode, the counter and reference electrodes were a platinum wire and an saturated calomel electrode (SCE) electrode, respectively. The ORR activity was carried out using rotating disk electrode (RDE) technique by linear sweep voltammetry (LSV) in the potential range of -1 to 0.2 V (vs. SCE) with a scan rate of 5 mV s^{-1} at different rotation rate from 400 to 2000 rpm in an O_2 -saturated 0.1 M KOH solution. Cyclic voltammetry (CV) curves were collected in the potential range of -1 to 0.2 V (vs. SCE) with a scan rate of 50 mV s^{-1} in an O_2 -saturated 0.1 M KOH solution. ORR stabilities of the catalyst was investigated by current vs time (i-t) chronoamperometric response of the PB-Fe and Pt/C during a constant potential at

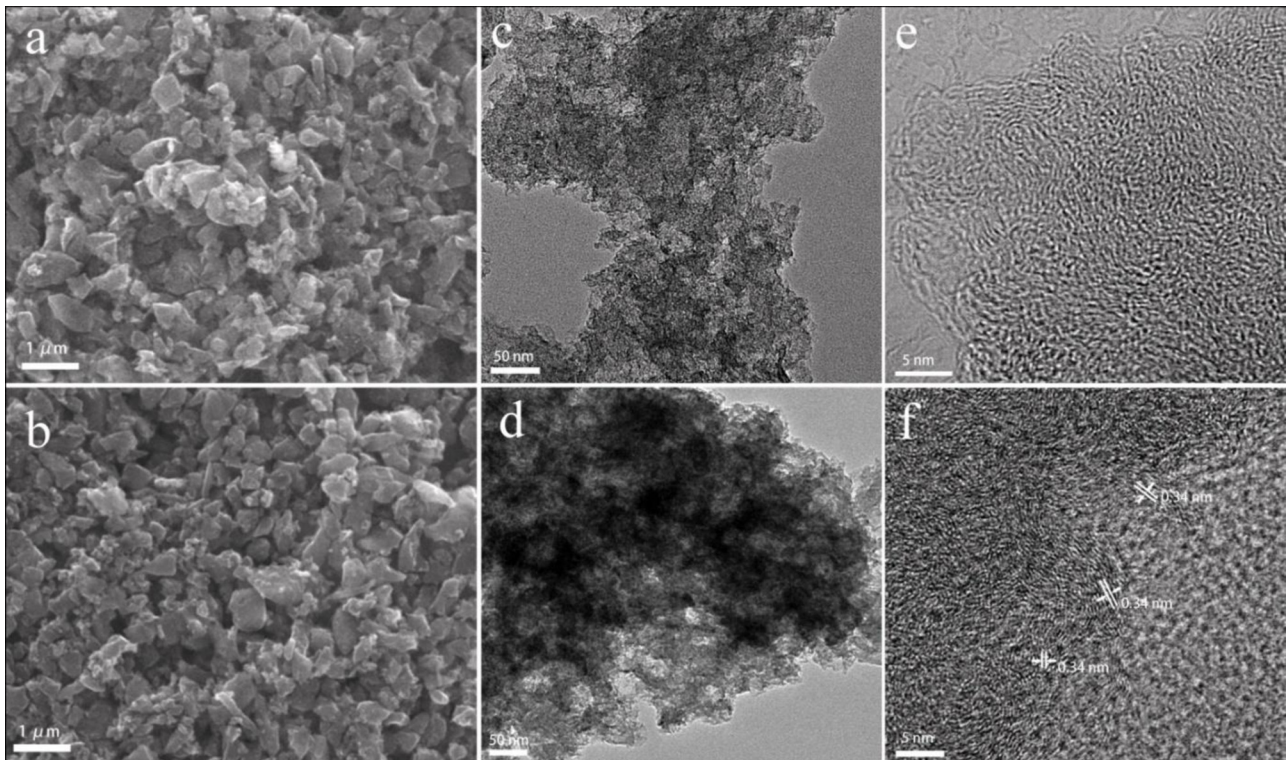


Fig. 1. FESEM and HRTEM images of CPB (a, c and e) and CPB-Fe (b, d and f).

−0.35 V at a rotation rate of 1600 rpm in O₂-saturated 0.1 M KOH. The tolerance of the catalysts were investigated by CV, LSV and i-t chronoamperometric response during a constant potential at −0.5 V in (O₂-saturated, O₂+CO (V_{CO}/V_{O₂}=10%) and O₂+3 M CH₃OH) 0.1 M KOH solution.

3. Result and discussion

Morphologies of the catalyst were investigated by means of FESEM and HRTEM. As shown in Fig. 1a and b, both CPB and CPB-Fe exhibit nearly identical morphologies, and the HRTEM images further show they possess rich porous structures (Fig. 1c and d). These suggest that such biology-derived carbon materials own a high specific surface area (see below). Fig. 1f shows graphitized carbon lattice fringes present in CPB-Fe, while obvious amorphous carbon remains in CPB (Fig. 1e), indicating the addition of trace iron can play an important role in forming graphitized structure carbon in terms of the catalytic function of iron at a lower temperature [18,19].

From the N₂ adsorption–desorption isotherms in Fig. 2a and b, CPB-Fe shows a higher BET specific surface area (641 m² g^{−1}) and a larger porosity than that of CPB (463 m² g^{−1}). These are mainly caused by the removal of iron oxides by acid leaching that leads to the formation of pore structures in CPB-Fe [19,20]. Enhanced ORR activity is expected because both the porous structure and high surface area can expose more active sites and benefit to the diffusion of ORR related species [1,12,21,22].

Raman spectra of the doped carbon catalysts are shown in Fig. 2c. The D peak (ca. 1340 cm^{−1}) and G peak (ca. 1590 cm^{−1}) are indicative of amorphous carbon and crystalline graphitic carbon, respectively [8,13,24]. And then the intensity ratio of the D to G bands (I_D/I_G) was used to estimate the graphitization degree of the samples [13,18,24]. Compared with CPB, CPB-Fe reveals a lower ratio of I_D/I_G , indicating the enhancement of graphitization degree with addition of iron, which is in good agreement with the HRTEM results. XPS patterns display the catalysts are predominantly composed of C, N and O (Fig. 2d and Table S1). The N1s spectra can be deconvoluted into four peaks related to four types of N species:

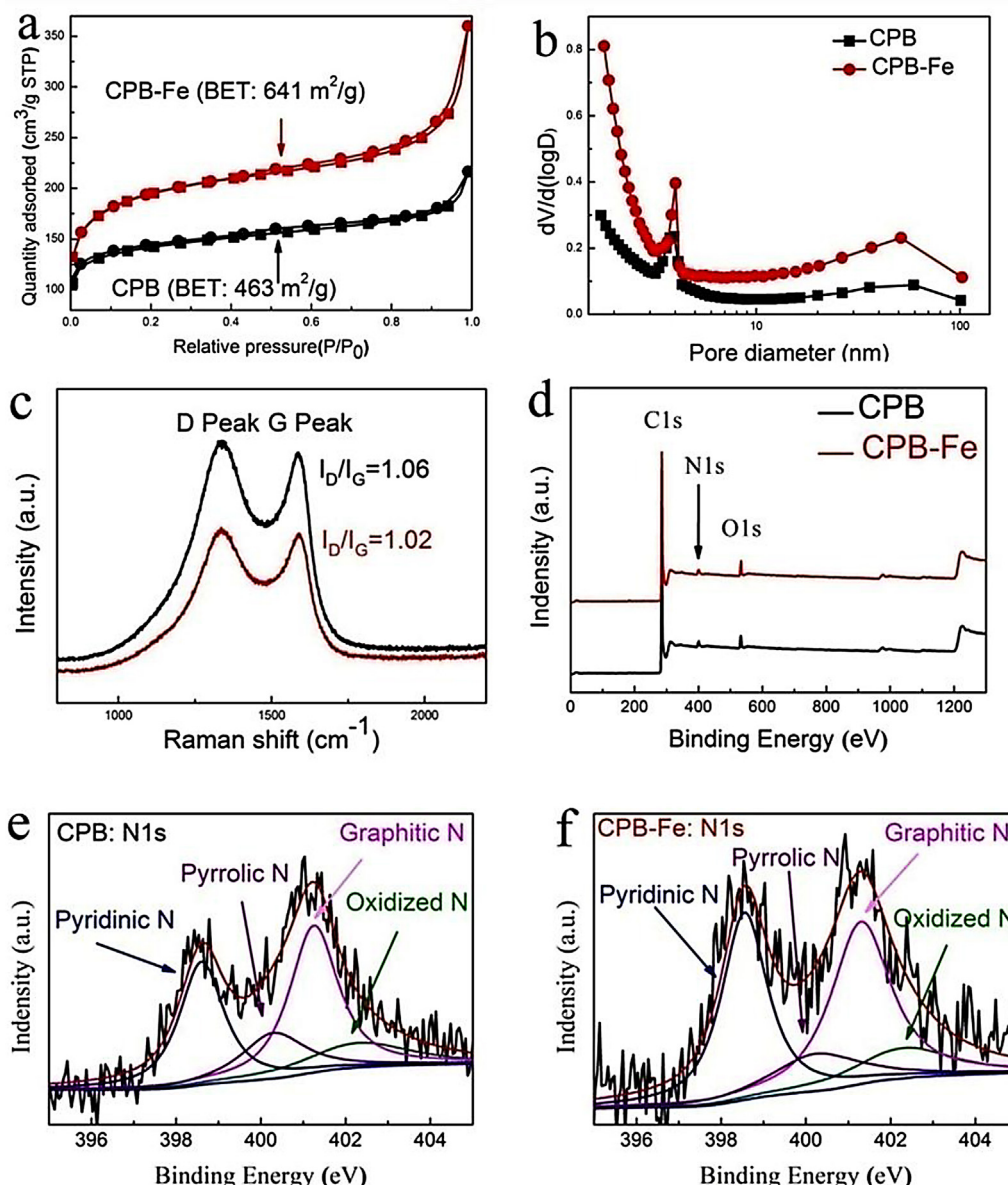


Fig. 2. N₂ adsorption–desorption isotherms (a), pore size distribution (b), Raman (c) and survey XPS spectra (d) of CPB, CPB-Fe catalysts, respectively; N1s spectra of CPB (e) and CPB-Fe (f).

the peak at 402.3 ± 0.3 eV, 401.1 ± 0.3 eV, 400.5 ± 0.3 eV and 398.2 ± 0.3 eV can be attributed to oxidized N, graphitic N, pyrrolic N, and pyridinic N, respectively (Fig. 2e and f) [5,8,10]. The fitted results exhibit the total content of N in CPB-Fe is slightly lower than CPB (Table S1), however the amounts of pyridinic N in CPB-Fe is higher than that of CPB due to the promotion of iron to forming pyridinic N at high temperatures [4,8,25]. Among them, graphitic

N could greatly increase the limiting current density, and pyridinic N could improve the onset potential and wettability, while other N species such as pyrrolic N and oxidized N have little impact on the electrochemical performance of carbon materials [4,5]. As reported, iron can promote the formation of the pyridinic and graphitic N at elevated temperatures [19]. The content of trace iron in CPB and CPB-Fe (0.212 and 0.938 wt%, respectively) was

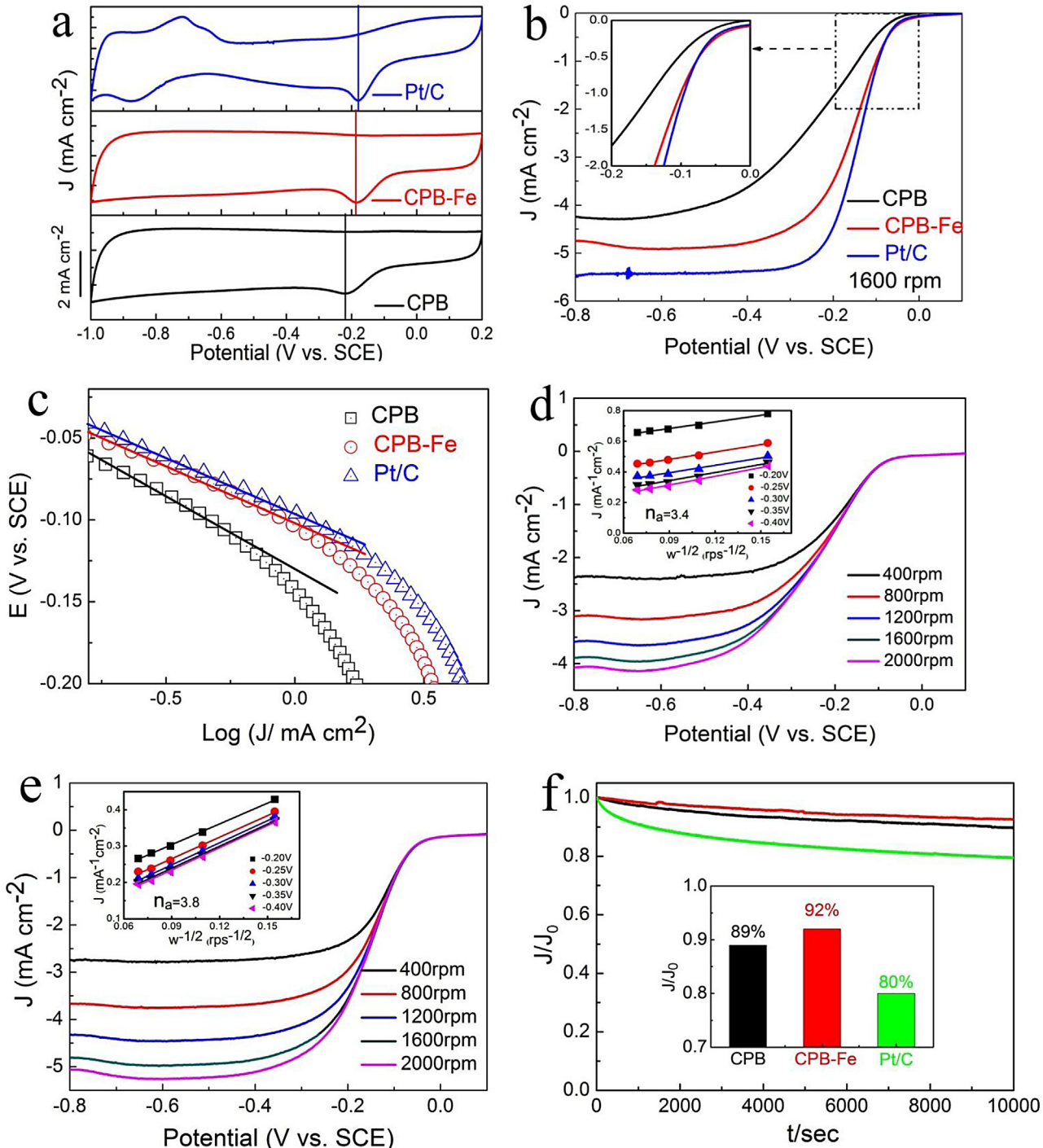


Fig. 3. Cyclic voltammetry (CV) and linear sweep voltammetry (LSV) curves for CPB, CPB-Fe, and commercial Pt/C catalysts (a and b); Tafel plots for CPB, CPB-Fe and Pt/C extracted from Fig. 3b (c); ORR polarization curves for CPL (d) and CPL-Fe (e) catalysts at different rotating rates, inset: K-L plots; i-t chronoamperometric responses of CPB, CPB-Fe and Pt/C catalysts in O_2 -saturated during a constant potential at -0.35 V (SCE) at a rotation rate of 1600 rpm; inset: the ratio of the J/J_0 (f). CV curves for all catalysts were tested in O_2 -saturated 0.1 M KOH solution with scanning rates of 50 mV s^{-1} ; LSV curves for all catalysts were tested in O_2 -saturated 0.1 M KOH solution with scanning rates of 5 mV s^{-1} and the rotation rate at 1600 rpm. E_{onset} was defined as the potential at which the ORR current is 5% of the limiting current density, $E_{1/2}$ was defined as the potential at which the ORR current is 50% of the limiting current density [23], respectively.

determined by inductively coupled plasma–atomic emission spectrometry. Hitherto, a large amount of literature has presented the preserved trace metal iron in catalysts can facilitate the electrocatalytic performance towards ORR [1,25–27].

Fig. 3a shows the CV curves of both CPB and CPB-Fe in O₂-saturated 0.1 M KOH solution. CPB exhibits a well-defined characteristic ORR peak centered at −0.22 V for O₂ reduction. After addition of iron into PB, the ORR peak of CPB-Fe is shifted to a more positive potential at −0.19 V, which is almost the same as the commercial Pt/C catalyst (−0.18 V). **Fig. 3b** also presents a more positive onset potential ($E_{\text{onset}} = -0.04 \text{ V}$), half-wave potential ($E_{1/2} = -0.16 \text{ V}$) and higher limiting current density ($LCD = 4.9 \text{ mA cm}^{-2}$) for CPB-Fe than that of CPB ($E_{\text{onset}} = -0.08 \text{ V}$, $E_{1/2} = -0.24 \text{ V}$ and $LCD = 4.3 \text{ mA cm}^{-2}$). Particularly, E_{onset} and $E_{1/2}$ of CPB-Fe are well comparable to that of Pt/C ($E_{\text{onset}} = -0.03 \text{ V}$, $E_{1/2} = -0.14 \text{ V}$), and as same as that of the reported N-doped carbon nanotubes and graphene catalysts (Table S2). Subsequently, Tafel slope (**Fig. 3c**) of CPB is 66 mV decade^{−1}, which is much lower than CPB (78 mV decade^{−1}) and very approaches Pt/C (63 mV decade^{−1}), implying the ORR mechanism of our catalysts is similar to the Pt-based catalyst in alkaline media. Based on the aforementioned characterization of the catalyst, the enhanced ORR activity of CPB-Fe can be attributed to the porous structure and high surface area, improved graphitization and high ratio of active N-containing species (pyridinic and graphitic N) [4,11,25].

To further understand the ORR mechanism of our catalysts, the ORR polarization curves at various rotating rates from 400 to 2000 rpm (**Fig. 3d, e**) were tested. The Koutecky-Levich (K-L) formula [13,25] (SI) was employed to calculate the average electron transfer number (n_a) based on the fact that the ORR current densities depend on the electrode rotation rates. According to the slope from the K-L plots (inset of **Fig. 3d, e**), the n_a value of CPB is 3.4, while the n_a of CPB-Fe is 3.8, which is very close to the 4 electron transfer number of Pt/C.

Fig. 3f shows the long-term testing results for CPB, CPB-Fe and Pt/C catalysts by recording the i-t chronoamperometric response in an O₂-saturated 0.1 M KOH solution. After 10,000 s, the current density attenuation for CPB and CPB-Fe is 5 and 3%, respectively. However, for Pt/C, the attenuation is up to 15%. The half-wave potential decay ($\Delta E_{1/2}$) of CPB, CPB-Fe and Pt/C catalysts before and after continuous potential cycles for 5000 times was also investigated, as shown in Fig. S2. $\Delta E_{1/2}$ of CPB and CPB-Fe is 15 and 11 mV, respectively, both of which is lower than that of Pt/C ($\Delta E_{1/2} = 29 \text{ mV}$). These results indicate the biology-derived doped carbon catalyst has a better electrochemical stability than the state-of-the-art Pt/C catalyst in alkaline media. The loss of the specific catalytic activity of Pt/C catalyst can be attributed to the migration and aggregation of Pt nanoparticles caused by continuous potential [1,3,9,27,28]. The excellent stability of the carbon catalyst can be predominantly attributed to the covalent bonding of the catalytically active heteroatom to the carbon framework, unlike the physical bonding of Pt over carbon supports [11,21,22]. In addition, the slightly higher stability of CPB-Fe than that of CPB can be attributed to the higher graphitization degree [8,10,25].

To investigate fuel crossover and poisoning impacts, we performed the electrocatalytic selectivity of catalysts against the electro-oxidation of methanol and CO by recording i-t chronoamperometric response. **Fig. 4a** shows CPB and CPB-Fe catalysts are insensitive to CO poisoning, whereas Pt/C is rapidly poisoned with a dramatically decreased current density. In addition, as shown in **Fig. 4b**, the current response of CPB and CPB-Fe remains unchanged after introduction of 3 M methanol into the O₂-saturated 0.1 M KOH solution, demonstrating they are insensitive to methanol. On contrary, Pt/C shows an instantaneous current jump upon the addition of methanol, reflecting sensitivity or low tolerance to

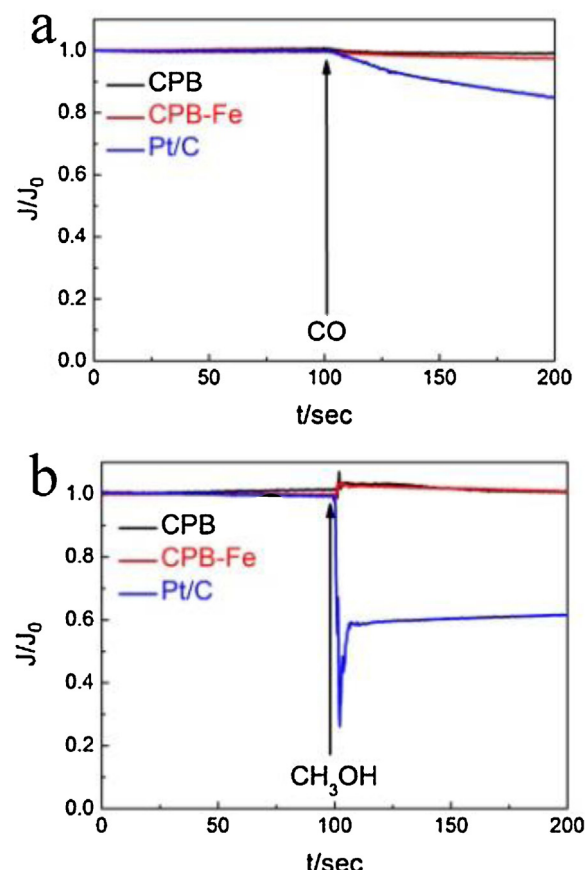


Fig. 4. i-t chronoamperometric responses of CPB, CPB-Fe and Pt/C in CO and O₂-saturated ($V_{\text{CO}}/V_{\text{O}_2} = 10\%$) (a) and 3 M methanol O₂-saturated (b) during a constant potential at −0.5 V (SCE) at a rotation rate of 1600 rpm in 0.1 M KOH.

methanol. The current lost of Pt/C is predominantly caused by the blockage of active sites on Pt nanoparticles by absorbing CO or methanol oxidation intermediate products [27,29]. It is reported that the adsorption energy (1.86 eV) of CO on Pt (111) surfaces is twice as large as that of O₂ (0.84 eV) [30]. These results reveal that the N-self-doped carbon catalyst has a significantly superior stability and immunity towards methanol crossover and CO poisoning than that of Pt/C, indicating a promising alternative to Pt-based catalyst for alkaline fuel cell at cathode.

4. Conclusions

We report a facile and high cost-effective method in fabricating a novel N-self-doped carbon-based ORR catalyst originated from pig blood. It is found that the addition of iron to the precursor can significantly enhance ORR performance of CPB-Fe due to the increased graphitization degree, surface area and active N species content as the self-N-doped carbon catalyst. In addition, the catalyst also shows superior stability and immunity for methanol crossover and CO poisoning in comparison with that of the commercial Pt/C catalyst. Thus, this study provides a very promising scenario to produce an eco-friendly and cheaper doped carbon catalyst for ORR, and even new application beyond fuel cells.

Acknowledgments

This work was supported financially by the National Natural Science Foundation of China (NSFC) (No. 51372186), and the

National Basic Research Development Program of China (973 Program) (No. 2012CB215504). The authors wish to thank Tingting Luo and Xiaoqing Liu at Materials Analysis Center of Wuhan University of Technology, for HRTEM (JEM-2100) measurement support.

Appendix A. Supplementary data

Supplementary data associated with this article can be found, in the online version, at <http://dx.doi.org/10.1016/j.electacta.2015.01.200>.

References

- [1] H.W. Liang, X. Zhuang, S. Bruller, X. Feng, K. Mullen, *Nat. Commun.* 5 (2014) 4973.
- [2] M. Lefevre, E. Proietti, F. Jaouen, J.P. Dodelet, *Science* 324 (2009) 71–74.
- [3] Y. Li, W. Zhou, H. Wang, L. Xie, Y. Liang, F. Wei, J.C. Idrobo, S.J. Pennycook, H. Dai, *Nat. Nanotech.* 7 (2012) 394–400.
- [4] N. Daems, X. Sheng, I.F.J. Vankelecom, P.P. Pescarmona, *J. Mater. Chem. A* 2 (2014) 4085–4110.
- [5] J.P. Paraknowitsch, A. Thomas, *Energy Environ. Sci.* 6 (2013) 2839–2855.
- [6] N. Ranjbar Sahraie, J.P. Paraknowitsch, C. Gobel, A. Thomas, P. Strasser, *J. Am. Chem. Soc.* 136 (2014) 14486–14497.
- [7] J. Jin, F. Pan, L. Jiang, X. Fu, A. Liang, Z. Wei, J. Zhang, G. Sun, *ACS Nano* 8 (2014) 3313–3321.
- [8] G. Wu, C.M. Johnston, N.H. Mack, K. Artyushkova, M. Ferrandon, M. Nelson, J.S. Lezama-Pacheco, S.D. Conradson, K.L. More, D.J. Myers, P. Zelenay, *J. Mater. Chem.* 21 (2011) 11392–11405.
- [9] W. Zhang, Z.Y. Wu, H.L. Jiang, S.H. Yu, *J. Am. Chem. Soc.* 136 (2014) 14385–14388.
- [10] J. Zhang, D.P. He, H. Su, X. Chen, M. Pan, S.C. Mu, *J. Mater. Chem. A* 2 (2014) 1242–1246.
- [11] J.Y. Cheon, T. Kim, Y. Choi, H.Y. Jeong, M.G. Kim, Y.J. Sa, J. Kim, Z. Lee, T.H. Yang, K. Kwon, O. Terasaki, G.G. Park, R.R. Adzic, S.H. Joo, *Sci. Rep.* 3 (2013) 2715.
- [12] X. She, D. Yang, D. Jing, F. Yuan, W. Yang, L. Guo, Y. Che, *Nanoscale* 6 (2014) 11057–11061.
- [13] Z. Mo, H. Peng, H. Liang, S. Liao, *Electrochim. Acta* 99 (2013) 30–37.
- [14] Y. Wang, A.B. Li, X.L. Chen, Y.Q. Han, J.J. Li, B.C. Xu, *Food Machinergy* 28 (2012) 272–274.
- [15] H.J. Wang, J. Xi, T. Liu, T. Chen, M.H. Ma, M. Zhang, A.L. Guo, *Meat Res.* 12 (2009) 81–87.
- [16] C.Z. Guo, W.L. Liao, C.G. Chen, *J. Power Sources* 269 (2014) 841–847.
- [17] C.Z. Guo, C.G. Chen, Z.L. Luo, *J. Power Sources* 245 (2014) 841–845.
- [18] Y. Hu, X. Zhao, Y. Huang, Q. Li, N.J. Bjerrum, C. Liu, W. Xing, *J. Power Sources* 225 (2013) 129–136.
- [19] J. Zhang, S. Wu, X. Chen, M. Pan, S. Mu, *J. Power Sources* 271 (2014) 522–529.
- [20] J. Zhang, S.Y. Wu, X. Chen, K. Cheng, M. Pan, S.C. Mu, *RSC Adv.* 4 (2014) 32811–32816.
- [21] N.K. Chaudhari, M.Y. Song, J.S. Yu, *Sci. Rep.* 4 (2014) 5221.
- [22] M.Y. Song, H.Y. Park, D.S. Yang, D. Bhattacharjya, J.S. Yu, *ChemSusChem* 7 (2014) 1755–1763.
- [23] L. Birry, J.H. Zagal, J.P. Dodelet, *Electrochim. Commun.* 12 (2010) 628–631.
- [24] S.C. Mu, H.L. Tang, S.H. Qian, M. Pan, R.Z. Yuan, *Carbon* 44 (2006) 762–767.
- [25] S. Ganesan, N. Leonard, S.C. Barton, *Phys. Chem. Chem. Phys.* 16 (2014) 4576–4585.
- [26] L. Wang, M. Pumera, *Chem. Commun.* 50 (2014) 12662–12664.
- [27] J. Liu, X. Sun, P. Song, Y. Zhang, W. Xing, W. Xu, *Adv. Mater.* 25 (2013) 6879–6883.
- [28] D. He, K. Cheng, T. Peng, X. Sun, M. Pan, S. Mu, *J. Mater. Chem.* 22 (2012) 21298–21304.
- [29] L. Wang, P. Yu, L. Zhao, C. Tian, D. Zhao, W. Zhou, J. Yin, R. Wang, H. Fu, *Sci. Rep.* 4 (2014) 5184.
- [30] P. Zhang, B.B. Xiao, X.L. Hou, Y.F. Zhu, Q. Jiang, *Sci. Rep.* 4 (2014) 3821.